Large-scale Heterogeneous Ultra-dense LEO Satellite-based Cellular Networks

Yuan Guo, Christodoulos Skouroumounis, and Ioannis Krikidis
IRIDA Research Centre for Communication Technologies
Department of Electrical and Computer Engineering, University of Cyprus
Email: {yguo0001, cskour03, krikidis}@ucy.ac.cy

***Abstract*—Owing to the growing demand for ubiquitous connectivity, low earth orbit (LEO) satellite-based communication networks are envisioned as a key-enabling technology for the next-generation networks. However, the existing literature disregards the heterogeneous nature of the real-world LEO satellite networks. Motivated by this, in this paper, an analytical framework based on stochastic geometry is developed, aiming to assess the downlink coverage performance of the large-scale heterogeneous LEO satellite-based communication networks. Based on the proposed mathematical framework, we derive the analytical expressions for the coverage probability, by taking into account the existence of inter-cell interference. Our results show that the inter-cell interference and fading channels jeopardize the coverage performance. Moreover, increasing the transmit power can improve the coverage probability at the low signal-to-noise ratio regime. Finally, we demonstrate that a higher coverage probability is achieved by narrowing the beam and/or by lowering the altitude of the LEO satellites.**

***Index Terms*—LEO satellites, stochastic geometry, interference, coverage performance, heterogeneous networks.**

I. Introduction

As one of the critical solutions for the sixth generation (6G) networks, low earth orbit (LEO) satellite-based communication system has recently attracted substantial attention from both industry and academia [1]. Over the past few years, around $4,700$ LEO satellites have been successfully launched by various companies, such as SpaceX, Amazon and OneWeb, aiming at providing satellite-based cellular service [2]. In contrast to the existing geostationary (GEO) satellites that are typically deployed at high altitude, the LEO satellites have many promising features and advantages over the GEO satellites, such as higher spatial flexibility, lower latency and lower deployment cost [3]. The potential benefits of the LEO satellite-aided networks have been extensively investigated in the literature [1]–[6]. Specifically, the authors in [1] present a comprehensive development roadmap of LEO satellite communication networks and study the unique advantages of applying LEO satellites over conventional terrestrial networks, such as high communication reliability, seamless global coverage and superior survivability. Moreover, the authors in [3] deal with an ultra-dense LEO satellite-based network, indicating that the network deployment with LEO satellites achieves larger capacity and lower latency compared to this one with the GEO satellites. Besides these benefits, the ultra-dense deployment of LEO satellites poses new challenges on the network modelling and analysis.

Recently the concept of stochastic geometry (SG) has been utilized for analysing the performance of LEO satellite-based communication systems, which is shown as a powerful and tractable mathematical tool for analysing the impact of key parameters on the network performance [4]–[6]. The authors in [4] investigate the coverage performance of the large-scale LEO satellites networks by assuming that the spatial deployment of satellites follows a homogeneous Poisson point process (PPP), while a practical satellite-to-ground (StG) path-loss model is proposed. This work is further extended in [5], where the optimal satellites' altitude for achieving the highest coverage probability is numerically demonstrated. Moreover, the authors in [6] study the downlink performance of LEO satellite-based systems by modelling the LEO satellites according to a homogeneous binomial point process (BPP), where an iterative algorithm is proposed to maximize the transmission rate and the system throughput. It should be noted that the fundamental performance of the LEO satellite-based networks is discussed in the aforementioned works, which are based on the assumption that large number of identical LEO satellites are deployed on the same altitude. In practice, the LEO satellite-based networks are highly-heterogeneous, i.e. various types of LEO satellites are generally deployed at different altitudes [1]–[3]. Moreover, the ultra-dense deployment of LEO satellites leads to the unprecedented increment of the interference, which is overlooked by the current literature.

Motivated by the above, in this work, we study the achieved performance of a large-scale heterogeneous ultra-dense LEO satellite-based network under the presence of inter-cell interference. More specifically, we investigate the downlink coverage performance for LEO satellite-based networks with a heterogeneous topology, where different types of LEO satellites are deployed on the different altitudes, and the locations of the LEO satellites are modelled according to multiple independent homogeneous PPPs. By leveraging tools from SG, we establish a tractable mathematical framework, where the coverage probability is analytically derived and the impact of several key network parameters on the network performance is discussed. Our results demonstrate that increasing the transmit power improves the coverage performance at the low signal-

This work was supported by the Research Promotion Foundation, Cyprus, under the project INFRASTRUCTURES/1216/0017 (IRIDA). This work was also supported by the European Research Council (ERC) under the European Union's Horizon 2020 research and innovation programme (Grant agreement No. 819819).

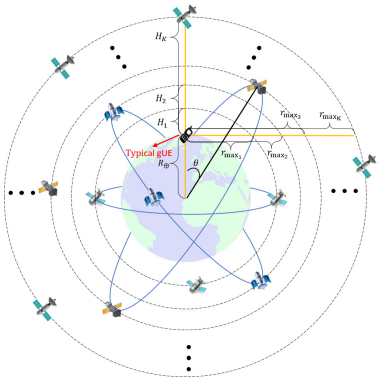

Fig. 1: Network topology of a K-tier LEO satellites network.

to-noise ratio (SNR) scenarios. In addition, the interference has a significant negative effect on the downlink coverage performance for the considered LEO satellite-based networks. Finally, it is illustrated that by narrowing the beamwidth or decreasing the altitude of the LEO satellites, the coverage probability can be significantly improved.

Notation: $\Gamma(\cdot)$ and $\gamma(\cdot,\cdot)$ denote the Gamma and the lower incomplete Gamma functions, respectively; ${}_1F_1(\cdot;\cdot;\cdot)$ is the confluent hypergeometric function of the first kind; $(n)!$ denotes the factorial of n; $(m)_z$ denotes the Pochhammer symbol; $\mathcal{H}(\cdot)$ denotes the Heaviside function.

II. System Model

A. Network model

We consider a multi-tier massive constellation setup as represented in Fig. 1, where LEO satellites are deployed at K different spherical surfaces concentric with the Earth, of altitudes H_k, with $H_k < H_{k+1}$, $\forall\ 1 \leq k \leq K-1$. For each tier constellation, the LEO satellites' locations are assumed to be distributed according to a homogeneous PPP, i.e. Φ_k with intensity $\lambda_k \approx \frac{N_k}{4\pi(R_\oplus+H_k)^2}$, where $R_\oplus$ is the Earth radius and N_k is the number of LEO satellites within the k-th tier constellation; while Φ_i and Φ_j for $i \neq j$ are independent [4]. We assume that all LEO satellites transmit signals with identical power P_t (dBW). In addition, we assume that the locations of the ground user equipments (gUEs) follow a uniform distribution. Without loss of generality and based on the Slivnyak's theorem, we perform our analysis for the typical gUE as shown in Fig. 1, while our results hold for any gUE in the network [7]. Let $x_{i,k}$ denote the location of the i-th LEO satellite of the k-th tier constellation, with distance $r_{i,k}$ from the typical gUE. Since gUEs can only receive the signals from the LEO satellites above their local horizons, the maximum distance between a gUE and a LEO satellite in the k-th tier is given by $r_{\max_k} = \sqrt{H_k^2 + 2H_kR_\oplus}$ [4]–[6].

B. Satellite-to-ground channel model

We assume that StG wireless channels experience both small-scale block fading and large-scale path-loss effect. Specifically, we adopt a well-known Shadowed-Rician model for the small-scale fading of the StG channels [2], [3], [6]. The cumulative distribution function (CDF) of the channel power gain is given by

$$F_h(x) = \left(\frac{2bm}{2bm+\Omega}\right)^m \sum_{z=0}^{\infty} \frac{(m)_z}{z!\Gamma(z+1)} \left(\frac{\Omega}{2bm+\Omega}\right)^z \times \gamma\left(z+1, \frac{1}{2b}x\right), \quad (1)$$

where Ω and $2b$ are the average power for the line of sight (LOS) and the multi-path components, respectively, m is the fading parameters based on the Nakagami-m fading channels, and $(m)_z = \frac{\Gamma(m+z)}{\Gamma(m)}$ is the Pochhammer symbol [6].

Regarding the large-scale fading, we adopt a practical StG path-loss model, which captures the blockage effects near the ground [4], [5]. More specifically, the path-loss between the typical gUE and the LEO satellite located at $x_{i,k}$ is given by $\ell(r_{i,k}, H_k) = \left(\frac{c}{4\pi f_c r_{i,k}}\right)^2 \xi(\theta_{i,k})$, where $\left(\frac{c}{4\pi f_c r_{i,k}}\right)^2$ is the free-space path-loss, f_c is the carrier frequency and $\xi(\theta_{i,k})$ is the excess gain which depends on the elevation angles, i.e. $\theta_{i,k}$. For the sake of simplicity, we approximate the excess gain as its mean value, which is given by

$$\bar{\xi}(\theta_{i,k}) = p_{\text{LoS}}(\theta_{i,k}) \exp\left(\frac{\rho^2\sigma_{\text{LoS}}^2}{2} - \rho\mu_{\text{LoS}}\right) + p_{\text{NLoS}}(\theta_{i,k}) \exp\left(\frac{\rho^2\sigma_{\text{NLoS}}^2}{2} - \rho\mu_{\text{NLoS}}\right), \quad (2)$$

where $\rho = (\ln 10)/10$, σ_{LoS}, σ_{NLoS}, μ_{LoS}, μ_{NLoS} are the parameters depending on the propagation environment, $\theta_{i,k} = \arccos((R_\oplus^2 + r_{i,k}^2 - (R_\oplus + H_k)^2)/(2r_{i,k}R_\oplus))$ is the Earth-centered zenith angle with respect to the LEO satellite located at $x_{i,k}$, and $p_{\text{LoS}}(\theta_{i,k}) = \exp(-\beta \sin\theta_{i,k}/(\cos\theta_{i,k} - \frac{R_\oplus}{R_\oplus+H_k}))$ is the probability of the LOS component [5], [8].

C. Sectorized antenna model

We assume that each LEO satellite generates a single beam perpendicular to the ground with beamwidth ψ_k, as shown in Fig. 2, while each gUE has single omnidirectional antenna. For the sake of simplicity, we approximate the actual beam pattern with a sectorized model. More specifically, the gUEs located within the main-lobe area of the LEO satellites' beam achieve an array gain equal to $G_{m,k}$, while the rest, experience an array gain equal to $G_{s,k}$ [4]–[6]. In addition, the main- and the side-lobe gains are given by $G_{m,k} \approx 32000/\psi_k^2$ and $G_{s,k} = \zeta G_{s,k}$, respectively, where ζ is the loss coefficient of the antenna directivity [9]–[12]. Hence, the antenna gain of the link between the typical gUE and the LEO satellite located at $x_{i,k}$ is given by

$$G_k(r_{i,k}) = \begin{cases} G_{m,k}, & r_{i,k} < R_{m,k} \\ G_{s,k}, & r_{i,k} \geq R_{m,k}, \end{cases} \quad (3)$$

where

$$R_{m,k} = (H_k + R_\oplus)\cos(\psi_k/2) - \sqrt{(H_k+R_\oplus)^2\cos^2(\psi_k/2) - H_k(H_k+2R_\oplus)},$$

represents the maximum distance between a gUE and a LEO satellite to locate within its main-lobe area. For LEO satellite scenarios with $H_k \ll R_\oplus$, we have $R_{m,k} \approx \frac{H_k}{\cos(\psi_k/2)}$.

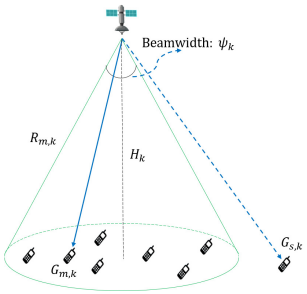

Fig. 2: Beamforming model for k-th tier LEO satellites, with beamwidth ψ_k, main- and side-lobe gains $G_{m,k}$ and $G_{s,k}$, respectively.

III. Heterogeneous LEO satellite-based cellular networks

We evaluate the coverage performance for the considered LEO satellite-based networks. Initially, we characterize the distribution of the distance from a gUE to its closest LEO satellite from each tier constellation. Then, we derive the association probability and the conditional distribution of the distance from a gUE to its serving LEO satellite. Finally, we evaluate the average aggregate interference power observed at the typical gUE and present the analytical expression for the downlink coverage probability.

A. Distance distribution

Let $r_{0,k}$ represent the Euclidean distance between the typical gUE and its closest LEO satellite that belongs in the k-th tier constellation. The probability density function (PDF) of $r_{0,k}$ is provided in the following Lemma.

Lemma 1. *The PDF of the distance from the typical gUE to the closest LEO satellite that belongs in the k-th tier constellation is given by*

$$f(r,\lambda_k,H_k)=\Lambda_k r\exp\left(-\frac{\Lambda_k(r^2-H_k^2)}{2}\right), \tag{4}$$

where $r\in[H_k,r_{\max_k})$ and $\Lambda_k=2\pi\lambda_k\frac{R_\oplus+H_k}{R_\oplus}$.

Proof. See Appendix A. □

Since StG wireless signals suffer from the significant path-loss due to the long propagation distance, we consider that each gUE communicates with its closest LEO satellite to maintain an acceptable received signal quality [2], [4]. The association probability is presented in the following Lemma.

Lemma 2. *A gUE is associated with a k-th tier LEO satellite with a probability that is given by*

$$\mathcal{A}_k=\sum_{i=k}^{K}\int_{H_i}^{H_{i+1}}\Lambda_k r\prod_{j=1}^{i}\exp\left(-\frac{\Lambda_j(r^2-H_j^2)}{2}\right)\mathrm{d}r, \tag{5}$$

where $H_{K+1}=r_{\max_K}$.

Proof. See Appendix B. □

To facilitate the analysis of the downlink coverage probability achieved by the considered network deployments, we provide the analytical expression for the conditional PDF of the contact distance, i.e. the distance from the typical gUE to its serving LEO satellite, in the following Lemma.

Lemma 3. *The PDF of the distance from the typical gUE to its serving satellite, i.e. $f(r|\mathcal{A}_k)$ is given by*

$$f(r|\mathcal{A}_k)=\sum_{i=k}^{K}\frac{\Lambda_k r\mathbb{1}(i,r)}{\mathcal{A}_k}\exp\left(-\sum_{j=1}^{i}\frac{\Lambda_j(r^2-H_j^2)}{2}\right), \tag{6}$$

where

$$\mathbb{1}(i,r)=\begin{cases}1, & \text{if } H_i\le r<H_{i+1}\\ 0, & \text{others.}\end{cases} \tag{7}$$

Proof. The proof follows a similar methodology as [13, Lemma 3], and thus it is omitted due to the space limitation. □

It is worth emphasising that by adopting different network parameters, the results provided in the aforementioned Lemmas hold for various network topologies. In particular, by assuming $H_k=H,\ \forall\ 1\le k\le K$, i.e. all LEO satellites are deployed at the same altitude, we obtain the conventional topology of heterogeneous networks for LEO satellite communication scenarios [13], while by selecting $H_k=H$, $\psi_k=\psi$ and $\lambda_k=\lambda,\ \forall\ 1\le k\le K$, we obtain the corresponding results for the single-tier LEO satellite networks that are investigated in [4], [5].

B. Coverage performance

We now investigate the downlink coverage performance of the considered LEO satellite-based heterogeneous networks. Initially, the average power of the interference observed at the typical gUE is evaluated in the following Proposition.

Proposition 1. *The average power of the aggregate interference observed at the typical gUE is given by*

$$\begin{aligned}\mathcal{I}(r_{0,k})=P_t(2b+\Omega)\kappa\sum\nolimits_{j=1}^{K}\Bigg(&\mathcal{H}(R_{m,j}-r_{0,k})\\ &\left(\int_{r_{0,k}}^{R_{m,j}}\Lambda_j\ell(r,H_j)G_{m,j}r\mathrm{d}r+\int_{R_{m,j}}^{r_{\max_j}}\Lambda_j\ell(r,H_j)G_{s,j}r\mathrm{d}r\right)\\ &+\int_{R_{m,j}}^{r_{\max_j}}\Lambda_j\ell(r,H_j)G_{s,j}r\mathrm{d}r\bar{\mathcal{H}}(R_{m,j}-r_{0,k})\Bigg),\end{aligned}$$

where $\mathcal{H}(\cdot)$ represents the Heaviside function [14], $\bar{\mathcal{H}}(\cdot)=1-\mathcal{H}(\cdot)$ and $\kappa\in[0,1]$ is the interference mitigation factor[1].

Proof. See Appendix C. □

We define the coverage probability as the probability that the signal-to-interference-plus-noise ratio (SINR) at the typical gUE is greater than a predefined threshold ω (dB), i.e. $\mathbb{P}\{\text{SINR}\ge\omega\}$. The analytical expression for the coverage probability is presented in the following Theorem.

[1] κ is used to capture the ability of practical protocols in reducing the co-channel interference. For the scenarios with $\kappa\to0$ as discussed in [2], the interference is totally removed, while $\kappa\to1$ represents the worst case, i.e. an interference mitigation scheme is not deployed.

$$\mathcal{P}_{c,k}(\omega) = \int_{H_k}^{R_{m,k}} \left(1 - F_h\left(\frac{\omega(\mathcal{I}(r)+\sigma^2)}{P_t G_{m,k}\ell(r,H_k)}\right)\right) f(r|\mathcal{A}_k)\mathrm{d}r + \int_{R_{m,k}}^{r_{\max_k}} \left(1 - F_h\left(\frac{\omega(\mathcal{I}(r)+\sigma^2)}{P_t G_{s,k}\ell(r,H_k)}\right)\right) f(r|\mathcal{A}_k)\mathrm{d}r. \quad (9)$$

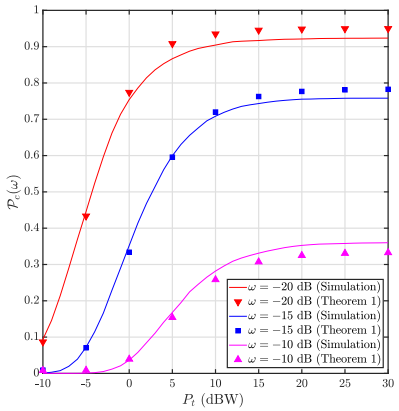

Fig. 3: Coverage probability versus the transmit power, for different decoding thresholds.

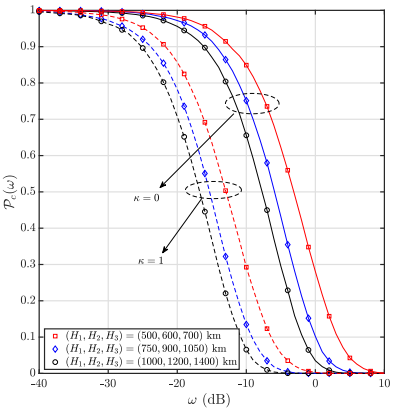

Fig. 4: Coverage probability versus the decoding threshold, for different interference mitigation factors and altitudes.

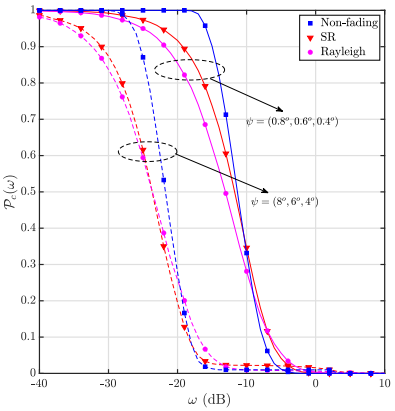

Fig. 5: Coverage probability versus the decoding threshold, for different types of fading channels and beamwidth.

Theorem 1. *The coverage probability is given by*

$$\mathcal{P}_c(\omega) \approx \sum\nolimits_{k=1}^{K} \mathcal{P}_{c,k}(\omega)\mathcal{A}_k, \quad (8)$$

where $\mathcal{P}_{c,k}(\omega)$ is given by (9) *and σ^2 represents the thermal noise power.*

Proof. See Appendix D. □

IV. Numerical Results

In this section, we provide simulation and theoretical results to validate the accuracy of our model, and to illustrate the impact of several key network parameters on the performance of the considered heterogeneous LEO satellite-based network. Unless other stated, in our results we use the following parameters: $K = 3$, $H_1 = 500$ km, $H_2 = 600$ km, $H_3 = 700$ km, $N_1 = 1000$, $N_2 = 800$, $N_3 = 600$, $\psi_1 = 0.8^o$, $\psi_2 = 0.6^o$, $\psi_3 = 0.4^o$, $R_\oplus = 6371$ km, $\sigma^2 = 3.6 \times 10^{-12}$, $\zeta = 0.01$, $P_t = 15$ dBW, $\beta = 2.3$, $\sigma_{\text{LoS}} = 2.8$ dB, $\sigma_{\text{NLoS}} = 9$ dB, $\mu_{\text{LoS}} = 0$ dB, $\mu_{\text{NLoS}} = 12$ dB, $f_c = 2$ GHz, $b = 0.158$, $m = 19.4$, $\Omega = 1.29$, $\kappa = 1$ [2], [5].

Fig. 3 illustrates the impact of the transmit power on the achieved coverage performance. In particular, Fig. 3 plots the coverage probability, $\mathcal{P}_c$, versus the transmit power P_t (dBW) for different decoding thresholds, i.e. $\omega \in \{-10, -15, -20\}$ dB. Firstly, we can observe that the coverage probability decreases with the increase of the decoding threshold. This was expected since by increasing the decoding threshold, the ability of a gUE to successfully decode the received signal reduces. Furthermore, we can easily observe that, the transmit power causes an increase of the coverage performance experienced by a gUE. This observation is due to the fact that, the increased transmit power leads to an enhanced intended signal strength, and thus improving the coverage probability. In addition, it is clear from the figure that the coverage probability asymptotically converges to a constant value. As expected, since as the transmission power of the transmitters increases, the noise is dominated by the inter-cell interference, leading to a constant coverage probability. Finally, the agreement between the theoretical results (markers) and the simulation results (curves) validates our mathematical analysis.

Fig. 4 depicts the effect of the interference and the constellations' altitudes on the achieved coverage performance. Specifically, Fig. 4 plots the coverage probability $\mathcal{P}_c$ versus the decoding threshold ω (dB) for different interference mitigation factors, i.e. $\kappa \in \{0, 1\}$ and different altitudes of the constellations, i.e. $(H_1, H_2, H_3) = (500, 600, 700)$ km, $(H_1, H_2, H_3) = (750, 900, 1050)$ km and $(H_1, H_2, H_3) = (1000, 1200, 1400)$ km. Initially, it can be observed that the interference has a significant negative impact on the network performance. More specifically, by taking into account the interference (i.e. $\kappa = 1$), the achieved coverage probability is much smaller than the non-interference scenario (i.e. $\kappa = 0$), which is investigated in [2], [6]. This can be explained based on the fact that, the gUEs suffer from the severe interference from other satellites due to the ultra-dense deployment of the LEO satellites, that degrades SINR observed at the gUEs. Hence, the interference mitigation techniques are essential for ensuring the communications quality of the ultra-dense LEO satellite-based networks. Moreover, we can easily observe that the coverage probability decreases with the increase of the constellations' altitudes. This was expected since higher altitudes of the constellations leads to a longer propagation distance between the gUEs and its serving satellites, which generally leads to a lower intended signal strength observed by the gUEs.

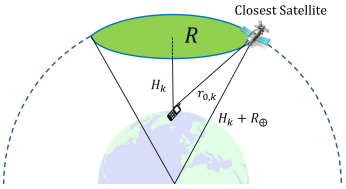

Fig. 6: The closest LEO satellite of the k-th tier constellation.

Fig. 5 shows the impact of the fading channels and the beamwidth on the coverage performance. In particular, Fig. 5 plots the coverage probability $\mathcal{P}_c$ versus the decoding threshold ω (dB) for different transmit beamwidth, i.e. $(\psi_1, \psi_2, \psi_3) = (0.8^o, 0.6^o, 0.4^o)$ and $(\psi_1, \psi_2, \psi_3) = (8^o, 6^o, 4^o)$. In addition, the Rayleigh and non-fading cases are numerically evaluated due to the space limitations. Note that for the Rayleigh fading case, the channel power gain follows an exponential distribution with unit mean, and for the non-fading case the channel power gain equals to one. Firstly, we can observe that by decreasing the beamwidth, the coverage probability is increased. This is based on the fact that by narrowing the beam more signal power can be focussed within the main-lobe area, i.e. the main-lobe antenna gain is increased which enhances the received signal strength and thus improves the coverage performance. Moreover, it can be observed that the fading channel jeopardizes the downlink performance, while the lowest coverage probability is obtained under the Rayleigh fading channel and the best performance is achieved for non-fading scenario. This was expected since Rayleigh fading models the multi-path propagation scenarios, e.g. gUE is located inside the buildings, thus resulting in the worst received signal quality.

V. Conclusion

In this paper, we studied the downlink coverage performance of the LEO satellites-based heterogeneous networks. By aiming to capture the heterogeneity of the practical LEO satellites-based networks, we considered a scenario where multi-tiers LEO satellites were deployed on the multiple constellations with different altitudes. In addition, by associating the gUE with its closest serving LEO satellite, we derived the corresponding association probability and the distribution of the contact distance. The coverage probability was analytically derived by leveraging tools from SG. Our results reveal that increasing the transmit power of the LEO satellites improves the coverage performance at the low SNR regime, while coverage probability converges to a constant value at high SNR regime. In addition, a narrower beam and a lower altitude of LEO satellites achieved a higher coverage probability. Moreover, the interference mitigation protocols were essential for the ultra-dense LEO satellites-based networks, due to the significant negative effect on the downlink networks. Finally, our established analytical framework can be widely used for modelling and analysing many other satellite-based networks, such as the LEO satellite-based cooperative network, while other more intelligent association schemes can also be explored for a potential interesting future work.

Appendix A
Proof of Lemma 1

The proof follows a similar approach as [4], [15]. We first compute the CDF of $r_{0,k}$ based on the null probability of PPP, i.e.

$$\begin{aligned} &F(r, \lambda_k, H_k) \\ =&\mathbb{P}\{r_{0,k} \leq r\} = 1 - \mathbb{P}\{r_{0,k} > r\} \\ =&1 - \mathbb{P}\{\text{no satellite of the } k\text{-th tier closer than } r\} \\ =&1 - \exp\left(-\lambda_k R(r, H_k)\right), \end{aligned} \tag{10}$$

where $R(r, H_k)$ represents the area of the spherical dome as shown in Fig. 6, which is given by

$$R(r, H_k) = \pi \frac{(r^2 - H_k^2)(R_\oplus + H_k)}{R_\oplus}.$$

Finally, by taking the derivative of $F(r, \lambda_k, H_k)$ with respect to r, i.e. $f(r, \lambda_k, H_k) = \frac{\partial}{\partial r} F(r, \lambda_k, H_k)$, the final expression in Lemma 1 is derived.

Appendix B
Proof of Lemma 2

The probability that the typical gUE is associated with k-th tier LEO satellite, is formulated as

$$\mathcal{A}_k = \mathbb{P}\left\{\min_{j, j\neq k} r_{0,j} > r_{0,k}\right\}. \tag{11}$$

Note that for the considered LEO satellites networks, $H_k \ll R_\oplus$, thus it is easily to show that $H_1 \leq H_2 \leq \cdots \leq r_{\max_1} \leq r_{\max_2} \leq \cdots \leq r_{\max_K}$. Hence, by applying the law of total probability and by denoting $r_{\max_K}$ as H_{K+1}, we can rewrite (11) as following

$$\mathcal{A}_k = \sum_{i=k}^{K} \mathbb{P}\left\{\min_{j, j\neq k} r_{0,j} \geq r_{0,k} \,\&\, H_i \leq r_{0,k} \leq H_{i+1}\right\}. \tag{12}$$

Then, by noticing that the terms $r_{0,k} \leq \min_{1\leq j\leq K-i} r_{0,i+j}$ hold for $H_i \leq r_{0,k} \leq H_{i+1}$, we have

$$\begin{aligned} &\mathbb{P}\left\{\min_{j, j\neq k} r_{0,j} \geq r_{0,k} \,\&\, H_i \leq r_{0,k} \leq H_{i+1}\right\} \\ =&\mathbb{P}\left\{\min_{\substack{1\leq j\leq i \\ j\neq k}} r_{0,j} \geq r_{0,k} \,\&\, H_i \leq r_{0,k} \leq H_{i+1}\right\} \\ =&\int_{H_i}^{H_{i+1}} \frac{\prod_{j=1}^{i} \exp\left(-\frac{\Lambda_j (r^2 - H_j^2)}{2}\right)}{\exp\left(-\frac{\Lambda_k (r^2 - H_k^2)}{2}\right)} f(r, \lambda_k, H_k) \mathrm{d}r \\ =&\int_{H_i}^{H_{i+1}} \prod_{j=1}^{i} \exp\left(-\frac{\Lambda_j (r^2 - H_j^2)}{2}\right) \Lambda_k r \mathrm{d}r. \end{aligned} \tag{13}$$

Finally, by substituting (13) into (12), the final result in Lemma 2 is derived.

APPENDIX C
PROOF OF PROPOSITION 1

Given that the typical gUE is associated with the k-th tier, the average power of the received interference is given by

$$\begin{aligned}\mathcal{I}(r_{0,k}) &= \mathbb{E}\left\{\sum\nolimits_{x_{i,j}\in\cup_{j=1}^{K}\Phi_j^{\setminus x_{0,k}}} \kappa P_t h_{i,j}\ell(r_{i,j},H_j)G_j(r_{i,j})\right\}\\ &\overset{(a)}{=}\mathbb{E}\left\{\sum\nolimits_{x_{i,j}\in\cup_{j=1}^{K}\Phi_j^{\setminus x_{0,k}}} \kappa P_t (2b+\Omega)\ell(r_{i,j},H_j)G_j(r_{i,j})\right\}\\ &\overset{(b)}{=}\sum_{j=1}^{K}\int_0^{2\pi}\int_\theta \kappa P_t(2b+\Omega)\ell(r,H_j)G_j(r)(R_\oplus+H_j)^2\sin\theta\mathrm{d}\theta\mathrm{d}\phi\\ &=\sum_{j=1}^{K}\int_\theta 2\pi\lambda_j\kappa P_t(2b+\Omega)\ell(r,H_j)G_j(r)(R_\oplus+H_j)^2\sin\theta\mathrm{d}\theta,\end{aligned}$$

where (a) is based on the fact that the channel power gain are independent and identically distributed random variables with mean $2b+\Omega$, and (b) follows from the Campbell's Theorem of PPP with the spherical coordinates [4], [7]. Then, by replacing θ with a function of r, i.e. $\theta = \arccos\left(\frac{R_\oplus^2+(R_\oplus+H_j)^2-r^2}{2R_\oplus(R_\oplus+H_j)}\right)$, we have

$$\begin{aligned}\mathrm{d}\theta =& \frac{r}{R_\oplus(h+R_\oplus)\sqrt{1-\frac{\left((H_j+R_\oplus)^2-r^2+R_\oplus^2\right)^2}{4R_\oplus^2(H_j+R_\oplus)^2}}}\mathrm{d}r,\\ \sin\theta =& \sqrt{1-\frac{\left((H_j+R_\oplus)^2-r^2+R_\oplus^2\right)^2}{4R_\oplus^2(H_j+R_\oplus)^2}}.\end{aligned}$$

Then we can obtain a compact expression of $\mathcal{I}(r_{0,k})$, i.e.

$$\begin{aligned}\mathcal{I}(r_{0,k}) =& \sum_{j=1}^{K}\int_{r_{0,k}}^{r_{\max_j}} \kappa\Lambda_j P_t(2b+\Omega)\ell(r,H_j)G_j(r)r\mathrm{d}r\\ =&\kappa P_t(2b+\Omega)\sum_{j=1}^{K}\mathcal{I}_j(r_{0,k}),\end{aligned} \tag{14}$$

where $\mathcal{I}_j(r_{0,k})$ is the interference from the j-th tier interfering LEO satellites, which is computed as

$$\begin{aligned}\mathcal{I}_j(r_{0,k}) =& \int_{R_{m,j}}^{r_{\max_j}} \Lambda_j\ell(r,H_j)G_{s,j}r\mathrm{d}r\bar{\mathcal{H}}(R_{m,j}-r_{0,k})\\ &+\int_{r_{0,k}}^{R_{m,j}} \Lambda_j\ell(r,H_j)G_{m,j}r\mathrm{d}r(R_{m,j}-r_{0,k})\\ &+\int_{R_{m,j}}^{r_{\max_j}} \Lambda_j\ell(r,H_j)G_{s,j}r\mathrm{d}r\mathcal{H}(R_{m,j}-r_{0,k}).\end{aligned} \tag{15}$$

Hence by substituting (15) into (14), the final result in Proposition 1 is proven.

APPENDIX D
PROOF OF THEOREM 1

By conditioning on $\mathcal{A}_k$, i.e. the typical gUE is associated with k-th tier LEO satellite, the coverage probability is given by

$$\begin{aligned}\mathcal{P}_{c,k}(\omega) =& \mathbb{P}\left\{\frac{P_t h_{0,k}G_k(r_{0,k})\ell(r_{0,k},H_k)}{\sum\limits_{x_{i,j}\in\cup_{j=1}^{K}\Phi_j^{\setminus x_{0,k}}}\kappa P_t h_{i,j}\ell(r_{i,j},H_j)G_j(r_{i,j})+\sigma^2}\geq\omega\right\}\\ \approx&\mathbb{P}\left\{h_{0,k}>\frac{\omega(\mathcal{I}(r_{0,k})+\sigma^2)}{P_tG_k(r_{0,k})\ell(r_{0,k},H_k)}\right\}\\ =&\int_{H_k}^{r_{\max_k}}\Big(1-F_h\Big(\frac{\omega(\mathcal{I}(r)+\sigma^2)}{P_tG_k(r)\ell(r,H_k)}\Big)\Big)f(r|\mathcal{A}_k)\mathrm{d}r\\ =&\int_{H_k}^{R_{m,k}}\Big(1-F_h\Big(\frac{\omega(\mathcal{I}(r)+\sigma^2)}{P_tG_{m,k}\ell(r,H_k)}\Big)\Big)f(r|\mathcal{A}_k)\mathrm{d}r\\ &+\int_{R_{m,k}}^{r_{\max_k}}\Big(1-F_h\Big(\frac{\omega(\mathcal{I}(r)+\sigma^2)}{P_tG_{s,k}\ell(r,H_k)}\Big)\Big)f(r|\mathcal{A}_k)\mathrm{d}r,\end{aligned}$$

where $F_h(\cdot)$ is the CDF of the channel power gain, which is given by (1). Finally, by applying the law of total probability, the final results in Theorem 1 is derived.

REFERENCES

[1] S. Liu, Z. Gao, Y. Wu, D. W. Kwan Ng, X. Gao, K.-K. Wong, S. Chatzinotas, and B. Ottersten, "LEO satellite constellations for 5G and beyond: How will they reshape vertical domains?" *IEEE Commun. Mag.*, vol. 59, no. 7, pp. 30–36, Jul. 2021.

[2] A. Talgat, M. A. Kishk, and M.-S. Alouini, "Stochastic geometry-based analysis of LEO satellite communication systems," *IEEE Commun. Lett.*, vol. 25, no. 8, pp. 2458–2462, Aug. 2021.

[3] R. Wang, M. A. Kishk, and M.-S. Alouini, "Ultra-dense LEO satellite-based communication systems: A novel modeling technique," *IEEE Commun. Mag.*, vol. 60, no. 4, pp. 25–31, Apr. 2022.

[4] A. Al-Hourani, "An analytic approach for modeling the coverage performance of dense satellite networks," *IEEE Wireless Commun. Lett.*, vol. 10, no. 4, pp. 897–901, Apr. 2021.

[5] ——, "Optimal satellite constellation altitude for maximal coverage," *IEEE Wireless Commun. Lett.*, vol. 10, no. 7, pp. 1444–1448, Jul. 2021.

[6] D.-H. Jung, J.-G. Ryu, W.-J. Byun, and J. Choi, "Performance analysis of satellite communication system under the shadowed-rician fading: A stochastic geometry approach," *IEEE Trans. Commun.*, vol. 70, no. 4, pp. 2707–2721, Apr. 2022.

[7] M. Haenggi, *Stochastic Geometry for Wireless Networks.* Cambridge University Press, 2012.

[8] A. Al-Hourani and I. Guvenc, "On modeling satellite-to-ground path-loss in urban environments," *IEEE Commun. Lett.*, vol. 25, no. 3, pp. 696–700, Mar. 2021.

[9] D.-H. Na, K.-H. Park, Y.-C. Ko, and M.-S. Alouini, "Performance analysis of satellite communication systems with randomly located ground users," *IEEE Trans. Wireless Commun.*, vol. 21, no. 1, pp. 621–634, Jan. 2022.

[10] G. Zheng, S. Chatzinotas, and B. Ottersten, "Generic optimization of linear precoding in multibeam satellite systems," *IEEE Trans. Wireless Commun.*, vol. 11, no. 6, pp. 2308–2320, Jun. 2012.

[11] K. Andreasson and R. Wallace, *Introduction to RF and Microwave Passive Components*. Artech, 2015.

[12] V. Petrov, M. Komarov, D. Moltchanov, J. M. Jornet, and Y. Koucheryavy, "Interference and SINR in millimeter wave and terahertz communication systems with blocking and directional antennas," *IEEE Trans. Wireless Commun.*, vol. 16, no. 3, pp. 1791–1808, Mar. 2017.

[13] H.-S. Jo, Y. J. Sang, P. Xia, and J. G. Andrews, "Heterogeneous cellular networks with flexible cell association: A comprehensive downlink SINR analysis," *IEEE Trans. Wireless Commun.*, vol. 11, no. 10, pp. 3484–3495, Oct. 2012.

[14] M. Di Renzo and W. Lu, "System-level analysis and optimization of cellular networks with simultaneous wireless information and power transfer: Stochastic geometry modeling," *IEEE Trans. Veh. Technol.*, vol. 66, no. 3, pp. 2251–2275, Mar. 2017.

[15] N. Okati, T. Riihonen, D. Korpi, I. Angervuori, and R. Wichman, "Downlink coverage and rate analysis of low earth orbit satellite constellations using stochastic geometry," *IEEE Trans. Commun.*, vol. 68, no. 8, pp. 5120–5134, Aug. 2020.